

PIBAL-576

~~PIBAL-576~~

576

CONTRACT NO. DA-30-069-ORD-2639  
ID 5506-59  
PBC 9-1361-91010-38002-3411/000  
SPB 24-109-59

AD 686330

THE THERMAL RESPONSE OF  
HEAT-SINK REENTRY VEHICLES

by

John D. C. Crisp and Peter Feitis



POLYTECHNIC INSTITUTE OF BROOKLYN

DEPARTMENT OF  
AERONAUTICAL ENGINEERING AND APPLIED MECHANICS

JULY 1960

Reproduced by the  
CLEARINGHOUSE  
for Federal Scientific & Technical  
Information Springfield Va. 22151

PIBAL REPORT NO. 576

38

Contract No. DA-30-069-ORD-2639  
ID 5506-59  
PBC 9-1361-91010-38002-3411/000  
SPB 24-109-59

THE THERMAL RESPONSE OF HEAT-SINK REENTRY VEHICLES

by

John D. C. Crisp and Peter Feitis

Polytechnic Institute of Brooklyn

Department of

Aerospace Engineering and Applied Mechanics

July 1960

PIBAL Report No. 576

## CONTENTS

	<u>Page</u>
1. Introduction.....	1
2. Notation.....	2
3. The Heat Transfer Equation.....	3
4. The Numerical Integration.....	4
5. Initial Conditions and Input Data.....	5
6. Multiple Pass Trajectories.....	6
7. Presentation of Results.....	7
8. Temperature-Time Histories.....	10
9. The Influence of Nose Geometry on Peak Wall Temperature.....	11
10. Conclusions.....	11
11. References.....	13
12. Acknowledgement.....	13

### 1. Introduction

In a performance comparison of reentry vehicles there are a number of important interrelated criteria determining the acceptability of the vehicle. These include the peak deceleration, the limits imposed by atmospheric heating, guidance control and accuracy, and time of descent. A general study has been undertaken which places emphasis on the first two considerations and is based on three vehicle configurations appropriate to both manned and unmanned entry into the earth's atmosphere from high supercircular speeds. The first vehicle type, designated "sphere" is a high drag, nonlifting body. The second, referred to below as the "body" type, is of moderate drag and possesses a trimming lift capability; while the third, the "wing", simulates low-drag, high lift vehicles. For each configurational type heat transfer behavior is to be assessed on the basis of three techniques of heat dissipation, viz., by radiation alone, by ablation or internal cooling, and by the utilization of the vehicle as a heat sink.

In this paper are presented the results of the heat sink studies in the form of thermal-time response and specifically in terms of temperature-time histories and peak temperatures as a function of vehicle mass, shape and aerodynamic parameters, entry orbit. The thermal response is correlated to peak deceleration.

The nose of each vehicle can be thought of as spherical and is defined by the nose radius  $R'$  and the wall thickness  $D$ . If  $R'$  and  $D$  are within certain bounds, the differential equation governing the temperature of the nose is essentially one-dimensional. The heat balance is dependent on the velocity and altitude of the vehicle at all times. These are known from earlier trajectory computations. For a representative range of single and multipass entry orbits there are presented peak temperature contours in the  $R'$ - $D$  plane which permit a choice of  $R'$ ,  $D$  combinations which for a given peak deceleration place limits on temperature.

In determining material constants appearing in the differential equation the heat shield is assumed to be manufactured of a so-called high performance material such as beryllium oxide ( $T_{max} = 5125^{\circ}R$ ).

2. Notation

A	= 25,688
B	= 1349.2
C <sub>0</sub>	= -7.348; C <sub>1</sub> = .10842; C <sub>2</sub> = -3.1476.10 <sup>-5</sup>
C <sub>3</sub>	= 56.25; C <sub>4</sub> = .0175
D	= 0.01 - 0.05 feet; thickness parameter, variable
E	= 0.21625.10 <sup>-12</sup> . T <sub>s</sub> <sup>4</sup> = .055303 (BTU/ft <sup>2</sup> sec)
e	eccentricity of ex-atmospheric ellipse
h	time step used in temperature calculations. (sec)
h'	time step used in trajectory calculations. (sec)(h=h'/N)
k	= 0.11856 · 10 <sup>9</sup> ft. <sup>3/2</sup> sec <sup>-1</sup> .
N	= h'/h
R	= 2 ft. - 12 ft.; variable vehicle parameter.
R	radial distance from the earth's center; non-dimensionalized with respect to r <sub>a</sub> .
R <sub>o</sub>	= .96957 = radius of spherical earth
r <sub>a</sub>	= 2.1556 · 10 <sup>7</sup> feet; radius of the initial condition (200 km.)
S	= 2 cal/min. cm. <sup>2</sup> = .1229 BTU/sec.ft. <sup>2</sup> ; solar constant
t	= t'( $\theta$ ) time in seconds in an elliptical orbit, measured from the line of apses.
t"	= t''(T) time in seconds (see "Multiple Pass Trajectories").
T <sub>w</sub>	= T/T <sub>s</sub> ; non-dimensionalized wall temperature of vehicle.
T	absolute wall temperature of vehicle.
T <sub>s</sub>	= 711.13 <sup>o</sup> R = (aS/E') <sup>1/4</sup> equilibrium temperature of the vehicle outside the atmosphere.

$v$  non-dimensional velocity =  $v/v_0$   
 $v_0$  initial velocity  $v$  at 200 km. altitude for which  $R=1$ .  
 $v$  absolute velocity (ft./sec.).  
 $v_0$  25,516 ft./sec.; circular orbital velocity at 200 km. altitude.  
 $v_s$  = 26,000 ft./sec.; normalizing factor for velocity used in temperature analysis.  
 $y$  altitude above sea-level (feet).  
 $y_e$  =  $0.65595 \cdot 10^6$  ft.; initial altitude (200 km.).  
 $\alpha$  = 0.45; vehicle coefficient of absorptivity.  
 $\alpha$  angle of incidence  
 $\beta$  =  $1/22,000 = .45455 \cdot 10^{-4}$  ft. $^{-1}$  scale height of the atmosphere.  
 $\tau$  = period of elliptical orbit  
 $w$  angular coordinate; true anomaly in Keplerian ellipse.  
 $\gamma$  flight path angle, positive upwards  
 $\gamma_0$  initial value of  $\gamma$ .

### 3. The Heat Transfer Equation

The one-dimensional differential equation governing the non-dimensional wall temperature  $T_w$  of the vehicle is:

$$\frac{dT_w}{dt} = \left\{ \frac{A'}{(R')^{1/2}} \left( \frac{v}{v_s} \right)^{13/4} [1 - 0.3 T_w/h_{se}] e^{-\beta y/2} - E' T_w^4 + \bar{\alpha} S \right\} \frac{1}{C(T_w) D}$$

This states that the heat transfer is a balance of forced convection heating (aerodynamic effects), thermal radiation (according to Planck's law) and solar irradiation. The source of the first term in this equation is Ref. (1), and it is seen to include the influence of surface temperature on the convective heating rate. A value of the solar constant  $S$  was found in Ref. (2). Other numerical data are listed in the Notation.

The coefficients of the differential equation depend on the time history of velocity  $v$  and altitude  $y$ ; and can be computed

from pre-calculated trajectories given in the form of  $V$ ,  $R$  (nondimensional velocity, radial distance) pairs at discrete time intervals.

#### 4. The Numerical Integration

The temperature equation can be integrated numerically by a Runge-Kutta technique (Ref. 3). In the procedure, an equation of the type  $dT/dt = f(t, T)$  is integrated using the well-known formulas:

$$T(t+h) = T(t) + 1/6(k_1 + 2k_2 + 2k_3 + k_4) ,$$

$$k_1 = hf(t, T); \quad k_2 = hf(t+h/2, T+k_1/2) ,$$

$$k_3 = hf(t+h/2, T+k_2/2); \quad k_4 = hf(t+h, T+k_3) .$$

The time step  $h$  must be chosen sufficiently small. The permissible value is determined by successively decreasing  $h$  until results become insensitive to variations in  $h$ .

In the present problem, the velocities  $V$  and altitudes  $y$  (or  $R$ ) which determine  $f(t, T)$ , are tabulated at time intervals  $h'$ . The time interval used in the trajectory calculations,  $h'$ , usually varies considerably during any given trajectory (Ref. 4). In the temperature calculations, the time step  $h$  was determined from the given time step  $h'$  by the relation  $h=h'/N$ ,  $N$  being an integer. Thus for  $N=1$ , the temperature is calculated at the same time intervals as the given velocity and altitude. The corresponding velocity and altitude are interpolated linearly between any two values. It was found by comparative calculations that parabolic or higher order interpolation between the table values was unnecessary.

The Runge-Kutta process was programmed for a Bendix G15 Computer, so that there are printed out six quantities for each integration step in the following order: (t) time in seconds; ( $T_w$ ) wall temperature nondimensionalized with respect to  $T_s = 711.13^{\circ}R$ ; (T) temperature in  $^{\circ}R$ ; (V) given nondimensionalized

velocity; ( $R$ ) given nondimensionalized distance from the earth's center;  $(dT/dt) = f(t, T)$  rate of change of nondimensionalized temperature. The time required to compute one temperature is approximately 50 seconds.

Comparative results indicate that the time step,  $h$ , used in the temperature calculations can be chosen equal to the given time step,  $h'$ , of the trajectory calculations which is related to the acceleration magnitude; i.e.,  $N=1$  is acceptable. The initial temperature of the vehicle, which must be prescribed, can be varied by as much as 10% without noticeably influencing the ensuing temperature history. The initial temperature (i.e., the temperature  $T_s = (2S/E')^{1/4}$  of a body in free space for which thermal equilibrium exists between solar irradiation and thermal reradiation) for all atmospheric passes was therefore fixed at  $T_s = 711.13^{\circ}R$ .

## 5. Initial Conditions and Input Data

### Initial Temperature:

For all calculations the chosen initial temperature was  $711.13^{\circ}R$ , which is based on an absorptivity  $\bar{\alpha} = 0.45$ .

### Time step:

The chosen time step was the one used in the trajectory calculations; this varied continuously<sup>(4)</sup> from 50 seconds prior to actual entry, through 5-10 seconds near entry, to a minimum of 2.5 seconds when decelerations are greatest.

### $R'$ (nose radius) - $D$ (thickness):

Each trajectory was run for several  $R'$  and  $D$  combinations in the range  $2 < R' < 6$  and  $.01 < D < .05$  ft. The combinations were chosen so as to delineate a peak temperature contour in the  $R' - D$  plane of close to  $5125^{\circ}R$ , the acceptable limit for a material such as beryllium oxide.

### "Sphere" - trajectories:

These trajectories carry the notation "S". All trajectories begin outside the effective limit of the earth's atmos-

sphere, i.e., at an initial value  $R=1$ . Two initial super-circular velocities were considered:  $V=1.3911$  and  $V=1.3088$ . This group includes nine single-pass trajectories, two double-pass, one triple-pass and one quadruple pass trajectory defined by a range of entry-angles.

"Body" - trajectories:

These trajectories carry the notation "B". These also have an initial  $R=1$ , and an initial velocity  $V=1.3911$ . This group is composed of fifteen trajectories including three skip trajectories of which nine lead to impact upon the first pass.

"Wing" - trajectories:

No temperature calculations have been made so far.

## 6. Multiple Pass Trajectories

In order to cater for multiple-pass trajectories, the machine storage of the given trajectory data  $V$ ,  $R$ ,  $t$  becomes excessive. It proves unnecessary anyway. Since the convection terms in the differential equation can be neglected outside the atmosphere, the equation can be integrated analytically. The result is:

$$t''(T) = (D/4E' T_s^3) \left\{ (a_0 + a_2 T_s^2) \log_e \left( \frac{T_w + 1}{T_w - 1} \right) + 2(a_0 - a_2 T_s^2) \tan^{-1}(T) \right. \\ \left. + a_1 T_s \log_e \left( \frac{T_w^2 + 1}{T_w^2 - 1} \right) - t''(1700) \right\},$$

where

$$(a_0, a_1, a_2) = (C_0, C_1, C_2) \quad \text{for} \quad 500^\circ < T < 1700^\circ$$

$$(a_0, a_1, a_2) = (C_3, C_4, 0) \quad \text{for} \quad 1700^\circ > T.$$

The time  $t'(w)$  along an elliptical orbit of eccentricity  $e$  and having a period  $\tau$  is (Ref. 5):

$$t' = \tau \frac{(1-e^2)^{1/2}}{2\pi} \left\{ \frac{-e \sin w}{1+e \cos w} + \frac{2}{(1-e^2)^{1/2}} \tan^{-1} \left[ \frac{(1-e^2)^{1/2}}{(1+e)} \tan(w/2) \right] \right\}$$

It is not possible to give an explicit relationship for the temperature in terms of exit angle. A plot of both  $t'(w)$  and  $t''(T)$  (for  $D=.02$ ) is given with which it is possible to determine the temperature of the vehicle at entry into the atmosphere at the end of an elliptical pass in free space. The information required for this is the temperature at exit, (i.e., at the beginning of the elliptical path) the eccentricity and the period of revolution of the ellipse. See Figs. 1, 2 and 3 and the Appendix.

A study of these graphs shows that for all practical purposes, the satellite vehicle cools off to essentially the equilibrium temperature,  $T_s = 711.13^{\circ}\text{R}$ , during its flight along the ellipse, irrespective of the temperature it had at the beginning of the ellipse. However, for flight times outside the atmosphere of less than about 10,000 sec. (for  $D=.02$ ) the temperature at reentry can be considerably higher than  $711.13^{\circ}\text{R}$ .

#### 7. Presentation of Results

Two forms of graphical presentation are given. The first (Figs. 4-10) consists of wall temperature-time histories and is designed to illustrate the typical effects of entry with and without lift, of initial velocity ( $V_0$ ) and entry angle ( $\gamma_0$ ), and of the loading ratio  $C_D \bar{S}/m$ . Temperature effects are related to trajectory type and the acceleration-time history or the peak deceleration. Figure 5 relates the heat transfer ( $dT/dt$ ) to temperature.

The second set of curves (Figs. 11-18) depicts the influence of vehicle nose radius ( $R'$ ) and skin thickness ( $D$ ) on peak temperature for a variety of initial velocities, entry angles,  $C_D \bar{S}/m$  ratios, and angles of incidence. Contours of constant peak wall temperature are given in the  $R'$ - $D$  plane. These were obtained by linear interpolation of peak temperatures at points of a mesh, some of which are shown in addition to the interpolated contours.

Some essential properties of the trajectories used for the heat transfer computations are summarized in Table I for the nonlifting vehicle and in Table II for the "body" with trimming lift capability. The latter is defined by the coupled lift-drag laws

$$C_L = Ma$$

$$C_D = C_{D_0} + Q \alpha^2$$

where  $M = \partial C_L / \partial \alpha$ ,  $C_{D_0}$ ,  $Q$  are varied constants and  $\alpha$  is the angle of incidence with  $\alpha_{max} = 30^\circ$ .

NONLIFTING VEHICLE ENTRY ( $\alpha=0$ ) FROM 200 Km.

INITIAL VELOCITY $V_0$	ENTRY ANGLE $-\gamma_0$	LOADING $(\frac{m}{C_D \bar{S}})$	ABSOLUTE ACCELERATION $A_{max.}$	TERMINAL CONDITION	SEE FIGURES
1.3911	8°	100 lb/ft <sup>2</sup>	1.3g	exit	5, 11
	8-1/4	100	2.8	exit	11
	8-1/2	100	7.6; 7.0	impact	11
	9	100	18.1	impact	5, 11
1.3911	8	25	3.4; 8.6	impact	4, 12
	8-1/4	25	8.0	impact	4, 12
	8-1/2	25	13.6	impact	4, 12
1.3088	7-1/2	100	1.3	exit	15
	8	100	8.9	impact	5, 15
	9	100	23.6	impact	5, 15
1.3088	7	25	1.02	exit	16
	7-1/2	25	3.3; 7.7	impact	16
	8	25	13.5	impact	16

TABLE I "S" Trajectories

LIFTING VEHICLE ENTRY ( $V_o = 1.3911$ ) FROM 200 km.

INCI- DENCE ANGLE $\alpha$	ENTRY ANGLE $-\gamma_o$	LOADING ( $\frac{m}{s}$ )	DRAG at $\alpha=0$ $C_{D_0}$	LIFT SLOPE $\frac{\partial C_L}{\partial \alpha}$	LIFT DRAG $C_L$ ( $\frac{C_L}{C_D}$ ) max	RELATIVE ACCELER- ATION $\bar{A}_{max}$	TERMINAL CONDI- TION	SEE FIGURES	
0	8°	25 lb/ft <sup>2</sup>	0.6	0.01	1	2.0g	exit	6,8,13	
	9	25	0.6	0.01	1	20.3	impact	6,7,13	
	12	25	0.6	0.01	1	53.8	impact	6,13	
	8	50	0.4	0.02	0.5	0.7	exit	14	
	9	50	0.4	0.02	0.5	17.1	impact	7,14	
	9	50	0.6	0.01	1	18.3	impact	7,14	
	9	25	0.4	0.02	0.5	19.1	impact	7,14	
	5°	8	25	0.6	0.01	1	1.8	exit	8,17
	9	25	0.6	0.01	1	15.0	impact	17	
	10°	8	25	0.6	0.01	1	1.6	exit	8,17
	9	25	0.6	0.01	1	12.2;5.1	impact	17	
	30°	8	25	0.6	0.01	1	1.6	exit	8,9,18
	9	25	0.6	0.01	1	8.7	exit	9,18	
	10	25	0.6	0.01	1	17.0;8.6; 3.4;1.2	impact	9,10,18	
	12	25	0.6	0.01	1	31.0;1.8; 1.1	impact	9,18	

TABLE II "B" Trajectories

A complete set of peak temperatures is given by Tables IV through XII. These formed the basis of the contours of Figs. 4 through 18.

### 8. Temperature-Time Histories

Entry without lift:

Figure 4. The effect of entry angle on trajectory ( $R'$ ), absolute wall temperature ( $T$ ), absolute acceleration.

$V_o = 1.3911$ ,  $C_D \bar{S}/m = 0.04$ ,  $\alpha = 0$ ,  $R' = 4$ ,  $D = 0.01$ .

Figure 5. The effect of initial velocity on trajectory ( $R'$ ), absolute wall temperature ( $T$ ), absolute acceleration.

$-\gamma_o = 8^\circ$  and  $9^\circ$ ,  $C_D \bar{S}/m = 0.01$ ,  $\alpha = 0$ ,  $R' = 6$ ,  $D = 0.04$ .

Figure 6. The alleviating effect of steep entry on peak wall temperature.  $V_o = 1.3911$ ,  $C_D \bar{S}/m = 0.024$ ,  $\alpha = 0$ ,  $R' = 4$ ,  $D = 0.03$ .

Figure 7. The effect of aerodynamic loading,  $C_D \bar{S}/m$ .  $V_o = 1.3911$ ,  $-\gamma_o = 9^\circ$ ,  $\alpha = 0$ ,  $R' = 6$ ,  $D = 0.05$ .

Entry with lift:

Figure 8. The effect of constant lift on wall temperature.  $V_o = 1.3911$ ,  $-\gamma_o = 8^\circ$ ,  $m/\bar{S} = 25 \text{ lb}/\text{ft}^2$ ,  $C_{D_o} = 0.6$ ,  $\partial C_L / \partial \alpha = 0.01$ ,  $(C_L / C_D)_{\max} = 0.5$ ,  $R' = 6$ ,  $D = 0.01$ .

Figure 9. The effect of entry angle at maximum lift.  $V_o = 1.3911$ ,  $\alpha = 30^\circ$ ,  $m/\bar{S} = 25 \text{ lb}/\text{ft}^2$ ,  $C_{D_o} = 0.6$ ,  $\partial C_L / \partial \alpha = 0.01$ ,  $(C_L / C_D)_{\max} = 0.5$ ,  $R' = 6$ ,  $D = 0.03$ .

Figure 10. Entry at maximum lift; the effect on temperature of nose geometry ( $R'$  and  $D$ ).  $V_o = 1.3911$ ,  $\alpha = 30^\circ$ ,  $-\gamma_o = 10^\circ$ ,  $m/\bar{S} = 25 \text{ lb}/\text{ft}^2$ ,  $C_{D_o} = 0.6$ ,  $\partial C_L / \partial \alpha = 0.01$ ,  $(C_L / C_D)_{\max} = 0.5$ .

## 9. The Influence of Nose Geometry on Peak Wall Temperature

Entry without lift:

Figure 11. The effect of entry angle.  $V_o = 1.3911$ ,  $\alpha = 0$ ,  $C_D \bar{S}/m = 0.010$ .

Figure 12. The effect of entry angle.  $V_o = 1.3911$ ,  $\alpha = 0$ ,  $C_D \bar{S}/m = 0.040$ .

Figure 13. The effect of steep entry.  $V_o = 1.3911$ ,  $\alpha = 0$ ,  $C_D \bar{S}/m = 0.024$ .

Figure 14. The effect of aerodynamic loading  $C_D \bar{S}/m$ .  $V_o = 1.3911$ ,  $\alpha = 0$ .

Figure 15. The effect of entry angle.  $V_o = 1.3088$ ,  $\alpha = 0$ ,  $C_D \bar{S}/m = 0.010$ .

Figure 16. The effect of entry angle.  $V_o = 1.3088$ ,  $\alpha = 0$ ,  $C_D \bar{S}/m = 0.040$ .

Entry with lift:

Figure 17. Low and moderate lift entry.  $V_o = 1.3911$ ,  $\alpha = 5^\circ$  and  $10^\circ$ ,  $-\gamma_o = 8^\circ$  and  $9^\circ$ .

Figure 18. Maximum lift entry.  $V_o = 1.3911$ ,  $\alpha = 30^\circ$ ,  $-\gamma_o = 8, 9, 10, 12^\circ$ .

## 10. Conclusions

- a. Temperature-time histories, and particularly peak temperature, are essentially independent of the entry equilibrium wall temperature for the practical range of entry conditions.
- b. For multiple-pass trajectories the vehicle reaches equilibrium temperature during the ex-atmospheric phase prior to reentry unless the ex-atmospheric trajectory is closely circular near the sensible limit of the atmosphere (100-120 km. altitude).
- c. Whereas with increasing entry angle the maximum deceleration increases rapidly, the peak wall temperature is fairly insensitive to entry angle, and moreover, the peak value rises to a maximum and then decreases.

- d. Lower initial entry velocities at the same entry angle may or may not lower the peak wall temperature and maximum deceleration.
- e. The effect of decreasing the aerodynamic loading  $m/C_D S$  lowers the peak wall temperature.
- f. The effect of entry with constant lift is to decrease slightly the peak temperature, monotonically with increasing incidence angle. Peak deceleration, however, can be drastically reduced at high incidence.
- g. "Skip" trajectories within the effective atmosphere can occur with or without lift. These are characterized by twin deceleration and temperature peaks (for a nonlifting entry) or by multiple deceleration peaks for a lifting entry. In the latter case there may be fewer temperature peaks than acceleration peaks. In any case subsequent peak values of temperature decrease in magnitude, although intervening temperatures usually remain moderately high. The first deceleration peak may or may not be critical; for nonlifting entry the second peak is often much larger; for lifting entry subsequent deceleration peaks are much smaller than the first for the cases presented here but this is by no means always so.
- h. Peak temperatures are relatively insensitive to the vehicle nose radius by comparison with the effect of skin thickness. The higher peaks occur of course with the smaller thicknesses; but the latter lead to lower exit or impact wall temperatures when heat loss due to reradiation occurs.
- i. The curves of Figures 11-18 suggest that for manned or unmanned entry to impact with acceptable decelerations a practical combination of nose radius ( $R'$ ) and skin thickness ( $D$ ) exists. For example, for manned entry with peak deceleration close to a 15g limit and peak wall temperature to about  $5000^{\circ}R$  reasonable  $R'-D$  combinations can be found for entry under the conditions given by Figs. 12-14, 16-18.

Of these perhaps the most desirable are Figs. 16 and 18. The former is a non-lifting ("S") entry from  $V_o = 1.3088$  with an  $8^\circ$  entry angle and  $C_D \bar{S}/m = 0.040$  while the latter is a "B" entry with maximum lift from  $V_o = 1.3911$  with a  $10^\circ$  entry angle and  $C_D \bar{S}/m = 0.036$ .

11. References

1. Kemp, N. H. and Riddell, F. R.: Heat Transfer of Satellite Vehicles Reentering the Atmosphere. Jet Propulsion, February 1957, Vol. 27, No. 2, Part I.
2. Goldberg and Pierce: Encyclopedia of Physics. Vol. 50, p. 3, 1959.
3. Scarborough, J. B.: Numerical Analysis. 3rd Edition, p. 299, 1955.
4. Crisp, John D. C.: On the Dynamics of Atmospheric Entry and Reentry. PIBAL Report No. 562, Polytechnic Institute of Brooklyn, April 1960.
5. Pohle, F. V. and Feitis, P.: Analysis of Central Force Systems in the Presence of Small Disturbing Forces. PIBAL Report No. 498, Polytechnic Institute of Brooklyn, 1959.

12. Acknowledgement

The authors are indebted to Dr. P. A. Libby for discussions and assistance in the formulation of this study.

APPENDIX

Ex-Atmospheric Temperature Response After Exit

Figures 1, 2 and 3 enable the determination of the time-temperature or the position-temperature relationship of the vehicle during ex-atmospheric motion between exit from and re-entry into the planetary atmosphere.

At exit the following quantities are required:

e eccentricity  
P nondimensionalized semi-latus rectum,  $p/r_a$   
 $\omega$  true anomaly  
 $T^x$  temperature at exit  
R exit altitude (nondimensionalized)

These quantities fix the ex-atmospheric flight time and so, for a given vehicle, the reentry temperature. To find the latter the following procedure can be used:

- (i) Compute the nondimensional semi-major axis  $A = P/(1-e^2)$ . Use Fig. 1 to find  $\tau$  the period of the ellipse.
- (ii) From Fig. 2 find the nondimensional time of flight  $\Delta t'/\tau$  using the exit value of  $\omega$  together with  $e$ .
- (iii) Then  $\Delta t' = (\Delta t'/\tau)\tau$ .
- (iv) In Fig. 3 locate the time  $(\frac{0.02t}{D} + 1000)$  corresponding to  $T^x$  and scale it for wall thickness  $D$  and so find  $t''$ .
- (v) To this time add  $\Delta t'$ . Normalize the resultant time to  $D = 0.02$ , i.e., recalculate  $(0.02t''/D + 1000)$  and read from Fig. 3 the reentry temperature. See also Table III.

T[ <sup>o</sup> R]	t"(T) (sec.)	T	t"(T) (sec.)
711.13	+ ∞	1700	0
711.2	30,034	1710	- 9.6250
711.5	24,281	1725	- 23.781
712	21,328	1750	- 46.422
720	13,318	1800	- 88.203
800	5604.6	1900	-159.88
900	3331.4	2000	-218.86
1000	2196.4	2130	-281.0
1100	1497.0	2200	-309.08
1200	1024.5	2300	-343.98
1300	688.39	2400	-373.80
1400	440.95	2500	-399.45
1500	254.40	3000	-486.19
1600	111.29	3550	-537.47
1650	52.223	4000	-562.80
1675	25.316	4500	-581.48
1690	9.9375	5000	-594.25
1700	0	71,150	-640.34

D = 0.02 feet

TABLE III

V = 1.3911

$-\gamma_0$ deg.	$C_{D_0}$ $\bar{S}/m$	R ft.	D ft.	$(\frac{dT}{dt})_{\max}$	Approx. $\Delta t_1$ sec	$T_{\max}$	$^{\circ}R$	Approx. $\Delta t_2$ sec	$g_{\max}$	TERMINAL CONDITION
8	0.01	2	0.01	0.119	60	6000		-10	1.3	EXIT
		2	0.03	0.0889	70	5500		-40		
		4	0.01	0.105	55	5490		-10		
		4	0.03	0.0735	70	4840		-50		
		6	0.04	0.0548	75	4090		-65		
8.25	0.01	2	0.01	0.142	55	6690		5	2.8	EXIT
		2	0.03	0.114	60	6320		-25		
		4	0.01	0.128	60	6130		-5		
		4	0.03	0.0964	70	5640		-35		
		6	0.04	0.0744	75	4940		-50		
8.5	0.01	2	0.01	0.165	55	7200		30	7.6	IMPACT
		2	0.03	0.142	45	6780		15		
		4	0.01	0.151	55	6540		20		
		4	0.03	0.121	55	6040		5		
		6	0.04	0.0959	60	5240		-10		
9	0.01	2	0.01	0.214	30	7630		20	18.1	IMPACT
		4	0.01	0.196	30	7000		10		
		2	0.03	0.194	30	6950		5		
		4	0.03	0.164	25	6070		5		
		6	0.04	0.132	30	5060		-5		

"S" TRAJECTORIES

$$\Delta t_1 = [\text{Time at } T_{\max}] - [\text{Time at } (\frac{dT}{dt})_{\max}]$$

$$\Delta t_2 = [\text{Time at } g_{\max}] - [\text{Time at } T_{\max}]$$

TABLE IV

V = 1.3911

$\gamma_0$ deg.	$C_{D_0}$	$\bar{S}/m$	R ft.	D ft.	$(\frac{dT}{dt})_{\max}$	Approx. $\Delta t_1$ sec	$T_{\max}$ 1st PEAK	$^{\circ}R$ 2nd	Approx. $\Delta t_2$ sec	$g_{\max}$ 1st PEAK	$g_{\max}$ 2nd PEAK	TERM- INAL CONDI- TION
8	0.04	2	0.01	0.123	60	5650	4380	-5	3.4	8.6		IMPACT
		2	0.02	0.101	50	5420	4240	-15				
		4	0.01	0.105	60	5170	4010	-5				
		2	0.03	0.086	70	5080	4060	-35				
		3	0.02	0.0920	60	5070	4000	-25				
		4	0.03	0.0686	80	4460	3620	-45				
8.25	0.04	2	0.01	0.136	40		6040		80	7.2		IMPACT
		2	0.02	0.121	40		5720		70			
		4	0.01	0.123	40		5500		80			
		3	0.02	0.110	50		5340		60			
		2	0.03	0.102	50		5300		50			
		4	0.03	0.0846	50		4620		50			
8.5	0.04	2	0.01	0.160	40		6230		10	13.6		IMPACT
		2	0.02	0.142	40		5810		-5			
		4	0.01	0.142	30		5680		10			
		3	0.02	0.127	40		5420		-5			
		2	0.03	0.122	40		5280		-15			
		4	0.03	0.101	40		4560		-15			

TABLE V

$$V = 1.3088$$

$\gamma_0$ deg.	$C_D$	$\bar{s}/m$	R ft.	D ft.	$(\frac{dT}{dt})$ max	Approx. $\Delta t_1$ sec	$T_{max}$	$^{\circ}R$	Approx. $\Delta t_2$ sec	$g_{max}$	TERMINAL CONDITION
7.5	0.01		2	0.01	0.0995	60	5770		-5	1.3	EXIT
			2	0.03	0.0759	85	5330		-40		
			4	0.01	0.0889	70	5280		-10		
			4	0.03	0.0627	75	4710		-50		
			6	0.04	0.0470	90	4000		-70		
8	0.01		2	0.01	0.144	55	6920		35	8.9	IMPACT
			2	0.03	0.126	45	6460		20		
			4	0.01	0.132	45	6340		35		
			4	0.03	0.107	45	5730		15		
			6	0.04	0.0842	60	4920		-5		
9	0.01		2	0.01	0.229	25	7500		20	23.6	IMPACT
			4	0.01	0.216	25	6820		20		
			2	0.03	0.202	30	6430		5		
			4	0.03	0.175	35	5590		5		
			6	0.04	0.137	30	4520		-5		

TABLE VI

$$V = 1.3088$$

$-\gamma_0$ deg.	$C_{D_0}$	$\bar{S}/m$	R ft.	D ft.	$(\frac{dT}{dt})_{\max}$	Approx. $\Delta t_1$ sec	$T_{\max}$ °R	Approx. $\Delta t_2$ sec	$g_{\max}$	TERMINAL CONDITION
7	0.04	2	0.01	0.0610	70	4180	-25	1.0	EXIT	
		3	0.01	0.0550	50	3920	-25			
		4	0.01	0.0520	60	3740	-35			
		2	0.02	0.0466	80	3710	-55			
		5	0.01	0.0494	60	3610	-35			
		3	0.02	0.0407	70	3410	-55			
		2	0.03	0.0365	90	3260	-75			
		2	0.04	0.0297	90	2900	-75			
		4	0.03	0.0282	90	2760	-75			
		7.5	0.04	0.0808	80	5430	-5	3.3*	IMPACT	
7.5	0.04	2	0.02	0.0868	60	5180	-25			
		4	0.01	0.0792	40	4950	-5			
		2	0.03	0.0729	80	4850	-45			
		3	0.02	0.0789	60	4850	-25			
		4	0.03	0.0584	90	4250	-65			
		8	0.04	0.139	30	5940	20	13.5	IMPACT	
8	0.04	2	0.02	0.124	30	5480	10			
		4	0.01	0.127	40	5370	10			
		3	0.02	0.114	40	5080	-5			
		2	0.03	0.106	40	4960	-5			
		4	0.03	0.0856	40	4240	-15			

\* second  $g_{\max} = 7.7$

TABLE VII

$$V = 1.3911 \quad \alpha = 0 \quad C_{D_0} \bar{S}/m = 0.024$$

$-\gamma_0$ deg	R ft.	D ft.	$(\frac{dT}{dt})_{\max}$	Approx. $\Delta t_1$ sec	$T_{\max}$	$^{\circ}R$	Approx. $\Delta t_2$ sec	$g_{\max}$	TERMINAL CONDITION
8	2	0.01	0.118	55	5840	0		2.0	EXIT
	6	0.01	0.0964	50	5050	-10			
	2	0.05	0.0653	80	4660	-55			
	4	0.03	0.0702	65	4650	-40			
	6	0.05	0.0446	90	3620	-75			
9	2	0.01	0.210	30	6930	10	20.3		IMPACT
	6	0.01	0.180	25	5920	10			
	4	0.03	0.141	30	4990	-5			
	2	0.05	0.132	30	4790	-10			
	6	0.05	0.0914	35	3580	-15			
12	2	0.01	0.450	10	7370	0	53.8		IMPACT
	6	0.01	0.376	10	6060	0			
	2	0.03	0.316	10	5260	-5			
	4	0.03	0.256	15	4380	-5			
	2	0.05	0.232	15	4060	-10			
	6	0.05	0.157	15	2960	-10			

"B" Trajectories

$$\Delta t_1 = [\text{Time at } T_{\max}] - [\text{Time at } (\frac{dT}{dt})_{\max}]$$

$$\Delta t_2 = [\text{Time at } g_{\max}] - [\text{Time at } T_{\max}]$$

TABLE VIII

$V = 1.3911$        $\alpha = 0$

$-\gamma_0$ deg	$C_D \bar{S}/m$	R ft.	D ft.	$(\frac{dT}{dt})_{\max}$	Approx. $\Delta t_1$ sec	$T_{\max}$	$\theta_R$	Approx. $\Delta t_2$ sec	$g_{\max}$	TERMINAL CONDITION
8	0.008	2	0.01	0.119	60	6010	-10	0.7		EXIT
		6	0.01	0.0975	55	5200	-15			
		2	0.05	0.0687	75	4840	-60			
		4	0.03	0.0734	70	4830	-50			
		6	0.05	0.0475	80	3740	-70			
9	0.008	2	0.01	0.215	35	7870	15	17.1		IMPACT
		6	0.01	0.190	30	6830	12			
		4	0.03	0.172	30	6340	0			
		2	0.05	0.163	35	6320	-5			
		6	0.05	0.121	35	4890	-10			
9	0.012	2	0.01	0.215	30	7520	15	18.3		IMPACT
		6	0.01	0.189	25	6500	10			
		4	0.03	0.162	30	5840	0			
		2	0.05	0.153	35	5740	-5			
		5	0.04	0.132	30	5040	-5			
		6	0.05	0.110	35	4380	-15			
9	0.016	2	0.01	0.212	>20	>7170	<20	19.2		IMPACT
		4	0.01	0.197	30	6640	10			
		3	0.02	0.189	25	6420	5			
		2	0.03	0.182	25	6340	0			
		6	0.01	0.184	25	6270	10			
		3.5	0.03	0.159	30	5650	-5			
		4	0.03	0.153	>25	>5380	<5			
		2	0.05	0.145	30	5340	-5			
		6	0.03	0.137	30	5010	-5			
		6	0.05	0.102	35	4040	-15			

TABLE IX

$$V = 1.3911 \quad C_D \bar{S}/m = 0.024$$

$-\gamma_0$ deg	$\alpha$	R ft.	D ft.	$(\frac{dT}{dt})_{\max}$	Approx. $\Delta t_1$ sec	$T_{\max}$ °R	Approx. $\Delta t_2$ sec	$g_{\max}$	TERMINAL CONDITION
8	5	2	0.01	0.118	55	5760	-5	1.8	EXIT
		6	0.01	0.0958	50	4970	-10		
		4	0.03	0.0692	65	4490	-45		
		2	0.05	0.640	80	4460	-60		
		6	0.05	0.0434	90	3430	-70		
9	5	2	0.01	0.209	30	6860	5	15.0	IMPACT
		6	0.01	0.179	25	5860	5		
		4	0.03	0.138	35	4980	-15		
		2	0.05	0.128	40	4830	-20		
		6	0.05	0.0889	45	3640	-30		
8	10	2	0.01	0.117	50	5700	-5	1.6	EXIT
		6	0.01	0.955	50	4900	-15		
		4	0.03	0.683	65	4360	-45		
		2	0.05	0.0628	70	4300	-55		
		6	0.05	0.0426	90	3280	-75		
9	10	2	0.01	0.205	25	6780*	5	12.2	IMPACT
		6	0.01	0.179	25	5790	0		
		4	0.03	0.135	35	4930	-20		
		2	0.05	0.125	40	4800	-30		
		6	0.05	0.0862	65	3650	-50		

\* 2nd peak  $T_{\max} = 3440$

TABLE X

$V = 1.3911$        $\alpha = 30$

$-\gamma_0$ deg	$D_0$ $\bar{S}/m$	R ft.	t ft.	$(\frac{dT}{dt})$ max	Approx. $\Delta t_1$ sec	$T_{max}$	$^{\circ}R$	Approx. $\Delta t_2$ sec	$g_{max}$	TERMINAL CONDITION
8	0.024	2	0.01	0.114	40	5480	-10	1.6	EXIT	
		4	0.01	0.103	45	4970	-15			
		3	0.02	0.0872	55	4720	-30			
		6	0.01	0.0938	50	4670	-15			
		2	0.03	0.0807	55	4630	-40			
		3.5	0.03	0.0678	65	4090	-50			
		4	0.03	0.0648	65	3980	-50			
		2	0.05	0.0590	80	3850	-65			
		6	0.03	0.564	65	3620	-50			
		6	0.05	0.0393	90	2890	-80			
9	0.024	2	0.01	0.205	25	6440	0	8.7	EXIT	
		4	0.02	0.152	30	5140	-15			
		2	0.04	0.129	40	4800	-30			
		6	0.02	0.136	30	4730	-20			
		2	0.05	0.112	50	4390	-40			
		6	0.03	0.108	45	4130	-35			
		4.5	0.05	0.0844	60	3570	-40			

TABLE XI

$$V = 1.3911 \quad \alpha = 30$$

				FIRST PEAK				SECOND PEAK						
$-\gamma_0$ deg	$C_D$ 0	$\bar{S}/m$	$R'$ ft.	$D$ ft.	$(\frac{dT}{dt})$ max	Appx $\Delta t_1$ sec	$T_{max}^R$ 0	Appx $\Delta t_2$ sec	$(\frac{dT}{dt})$ max	Appx $\Delta t_1$ sec	$T_{max}$	Appx $\Delta t_2$ sec	TERMINAL CONDI- TION	
10	0.024			2	0.01	0.287	20	6740	0	0.0818	20	4230	-5	IMPACT
				6	0.01	0.238	15	5640	-5	0.0628	25	3490	-10	
				4	0.02	0.206	25	5160	-15	0.0434	25	3290	-15	
				6	0.02	0.183	25	4720	-15	0.0373	25	3070	-15	
				2	0.04	0.172	35	4700	-25	0.0308	35	3350	-25	
				4	0.03	0.164	35	4460	-25	0.0304	35	3100	-25	
				2	0.05	0.149	45	4250	-35	0.0248	35	3280	-25	
				6	0.03	0.144	35	4040	-25	0.0257	35	2920	-25	
				4.5	0.05	0.112	45	3440	-35	0.0178	35	2900	-25	
				6	0.05	0.100	45	3180	-35	0.0158	35	3100	-25	
				$g_{max}^1 = 17.0$				$g_{max}^2 = 8.6$				$g_{max}^3 = 3.4$		$g_{max}^4 = 1.2$

12	0.024	4	0.02	0.288	15	4990	-10	0.0178	20	2760	-5	IMPACT	
		6	0.02	0.254	20	4530	-10	0.0146	20	2640	-5		
		2	0.04	0.235	20	4400	-15	0.0105	20	3060	-5		
		6	0.03	0.196	20	3770	-15	0.0089	15	2690	-5		
		4.5	0.05	0.151	30	3150	-25	0.0063	15	>2690	-5		
				$g_{max}^1 = 34.1$				$g_{max}^2 = 9.5$				$g_{max}^3 = 1.8$	

TABLE XII

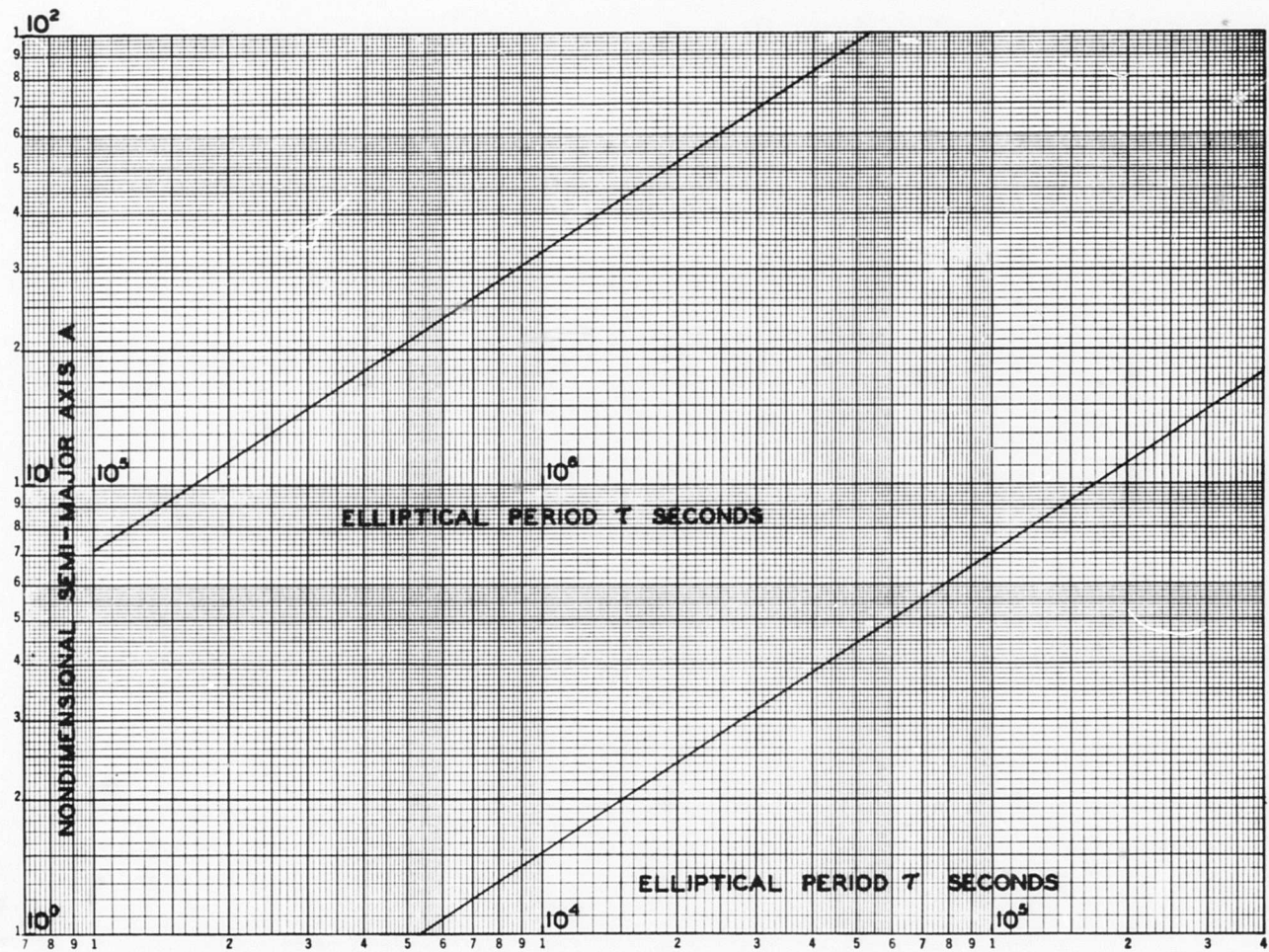


FIG. 1 MAJOR AXIS & PERIOD OF KEPLERIAN ELLIPSE

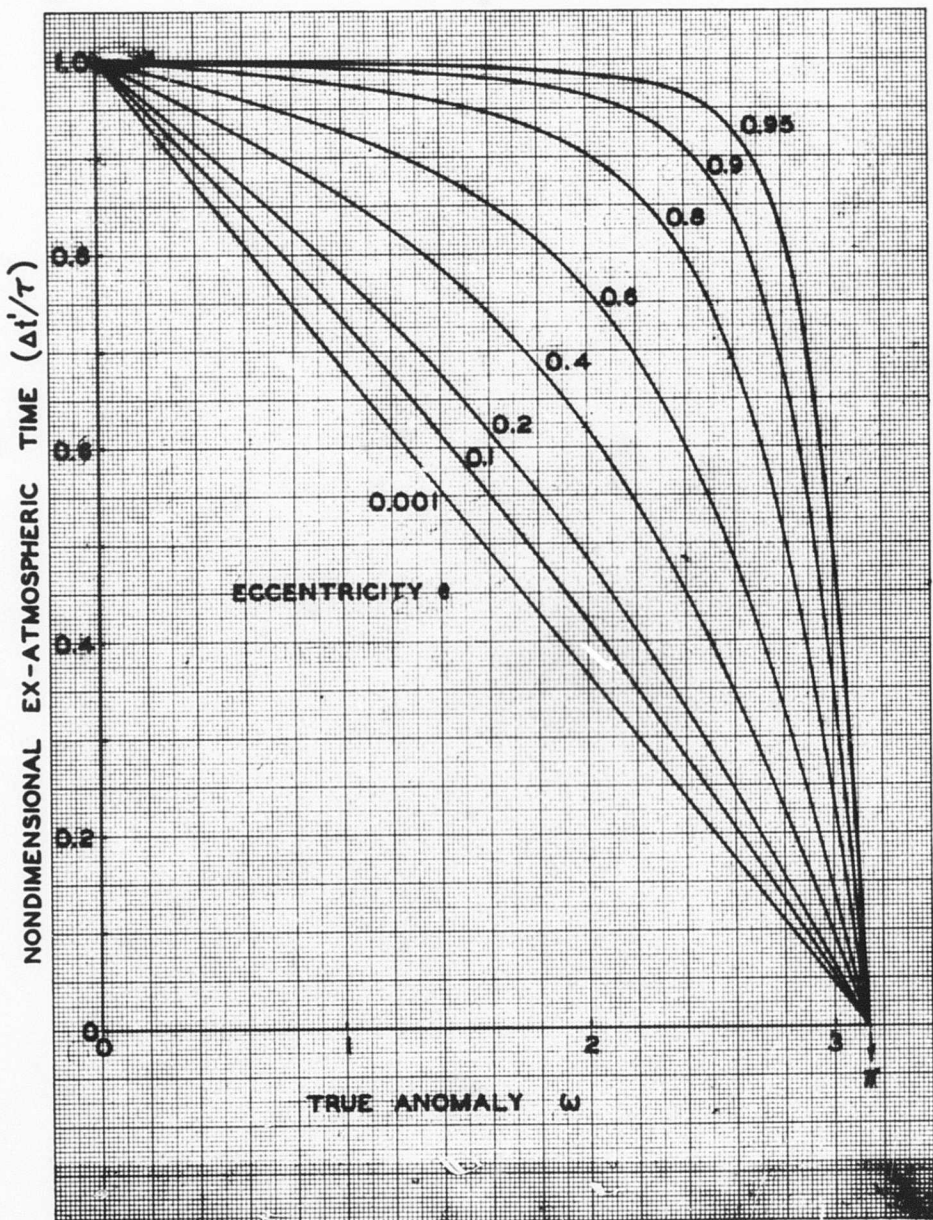


FIG. 2 EX-ATMOSPHERIC FLIGHT TIME IN TERMS OF EXIT CONDITIONS

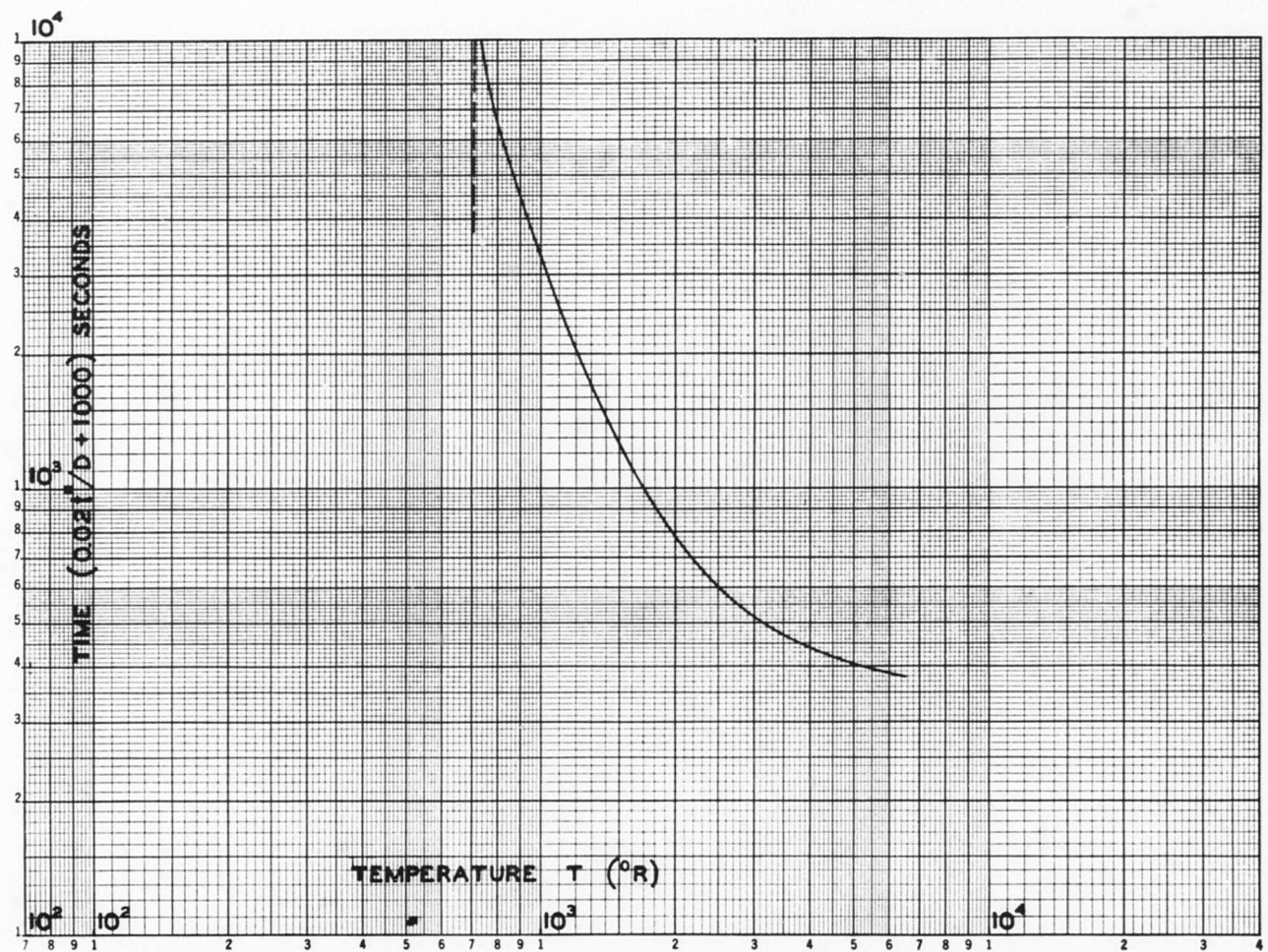


FIG. 3 REENTRY TEMPERATURE AND EX-ATMOSPHERIC FLIGHT TIME

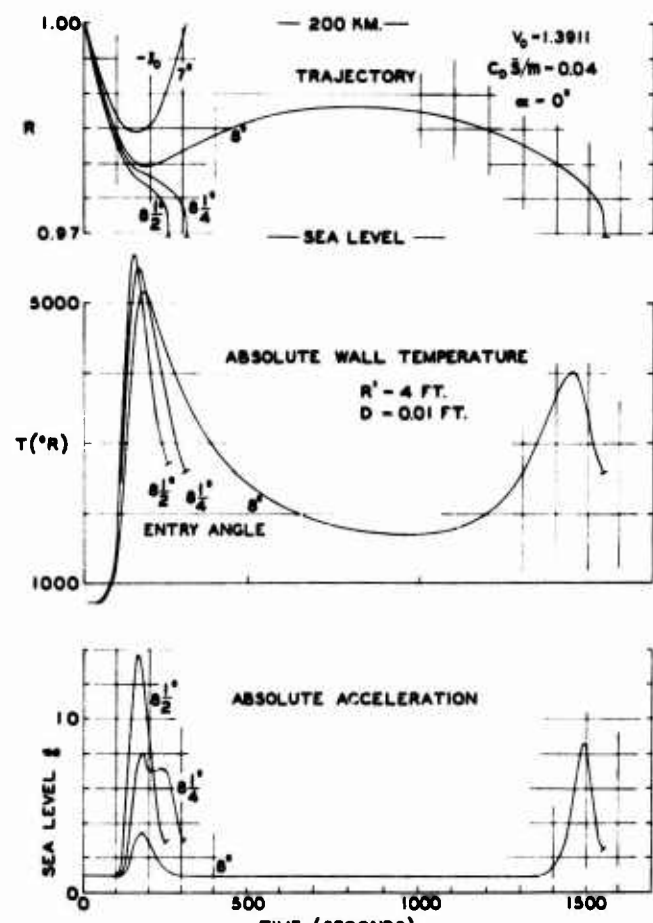


FIG. 4 EFFECT OF ENTRY ANGLE ON WALL TEMPERATURE AND DECELERATION

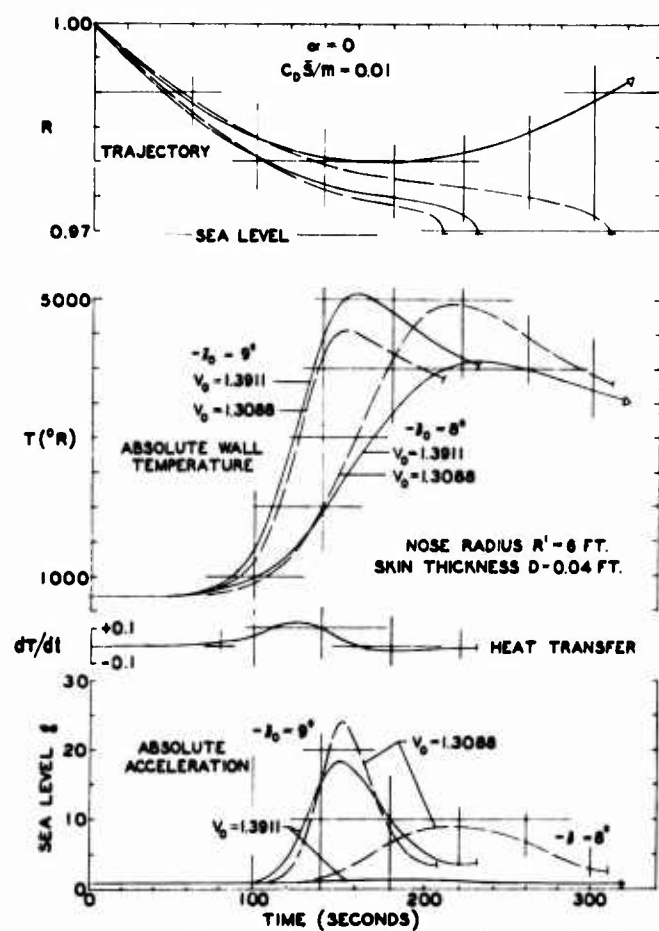


FIG. 5 EFFECT OF ENTRY VELOCITY ON WALL TEMPERATURE AND DECELERATION

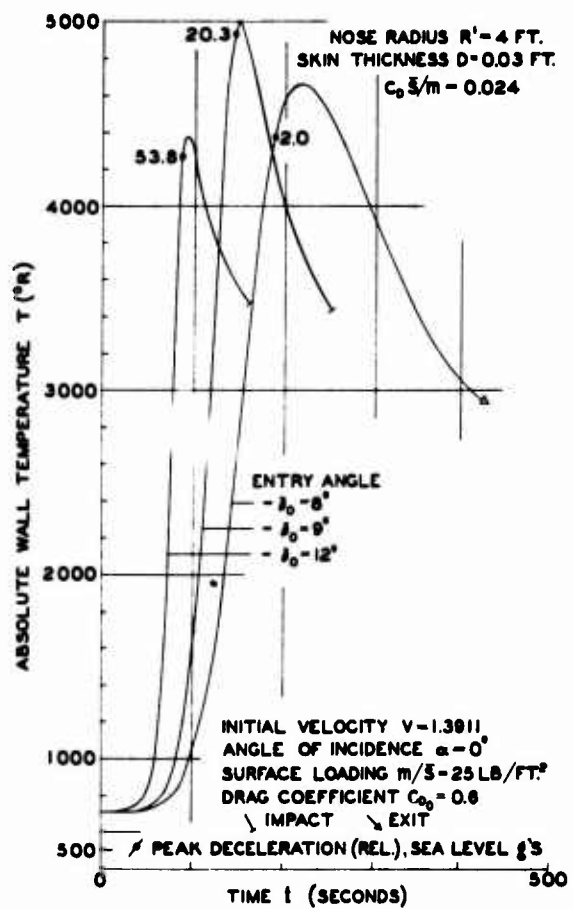


FIG. 6 ALLEVIATING EFFECT OF STEEP ENTRY  
ON WALL TEMPERATURE

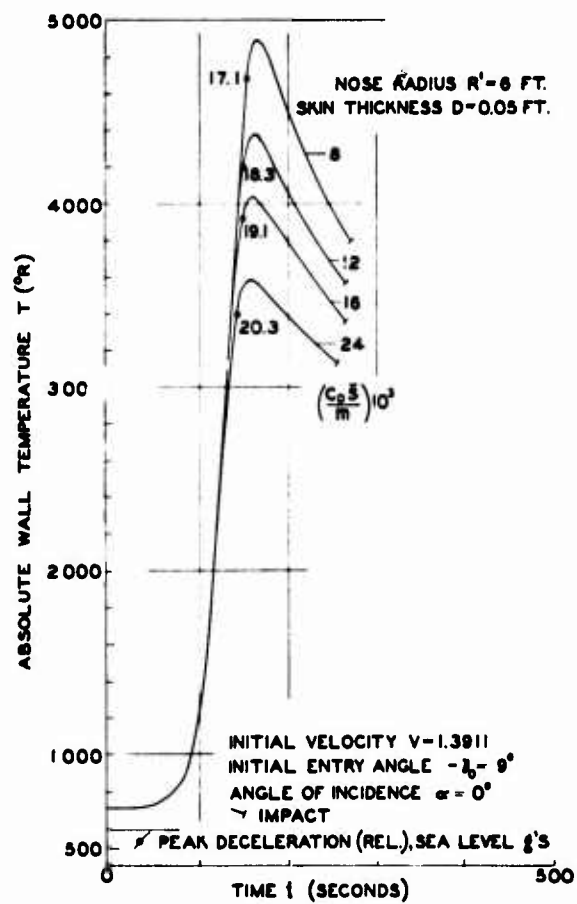


FIG. 7 EFFECT OF SURFACE LOADING  $m/C_0 S$   
ON WALL TEMPERATURE

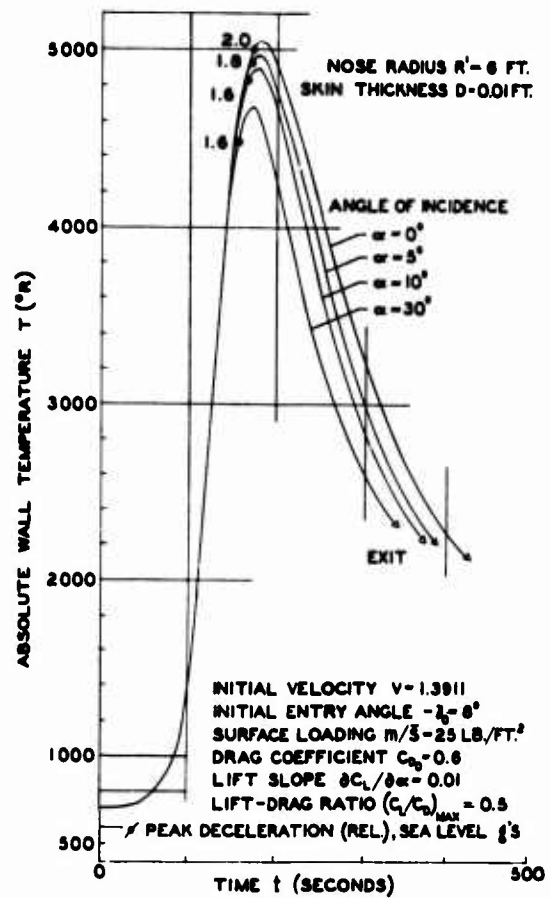


FIG. 8 EFFECT OF CONSTANT LIFT  
ON WALL TEMPERATURE

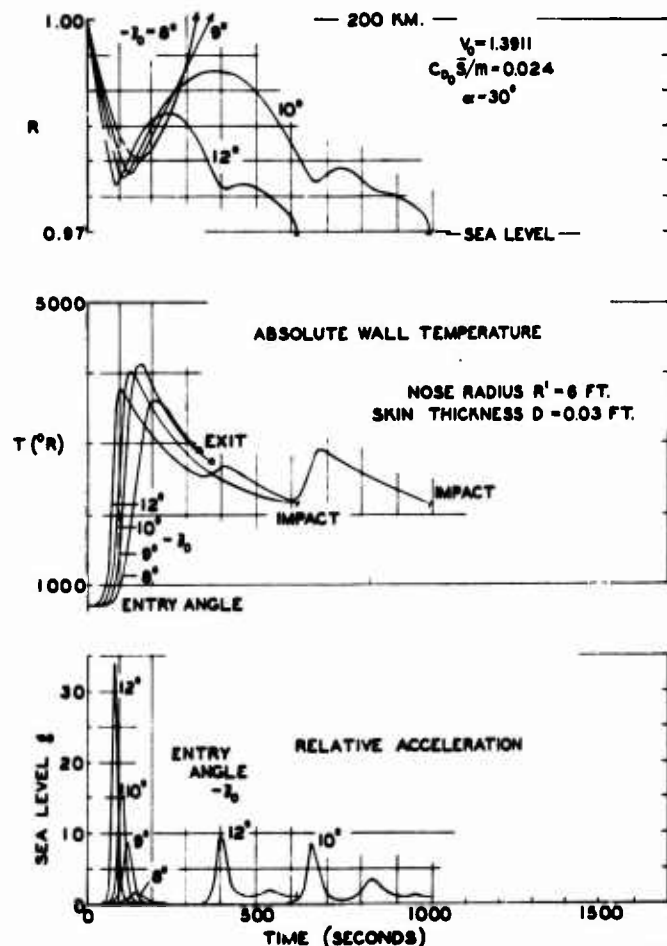
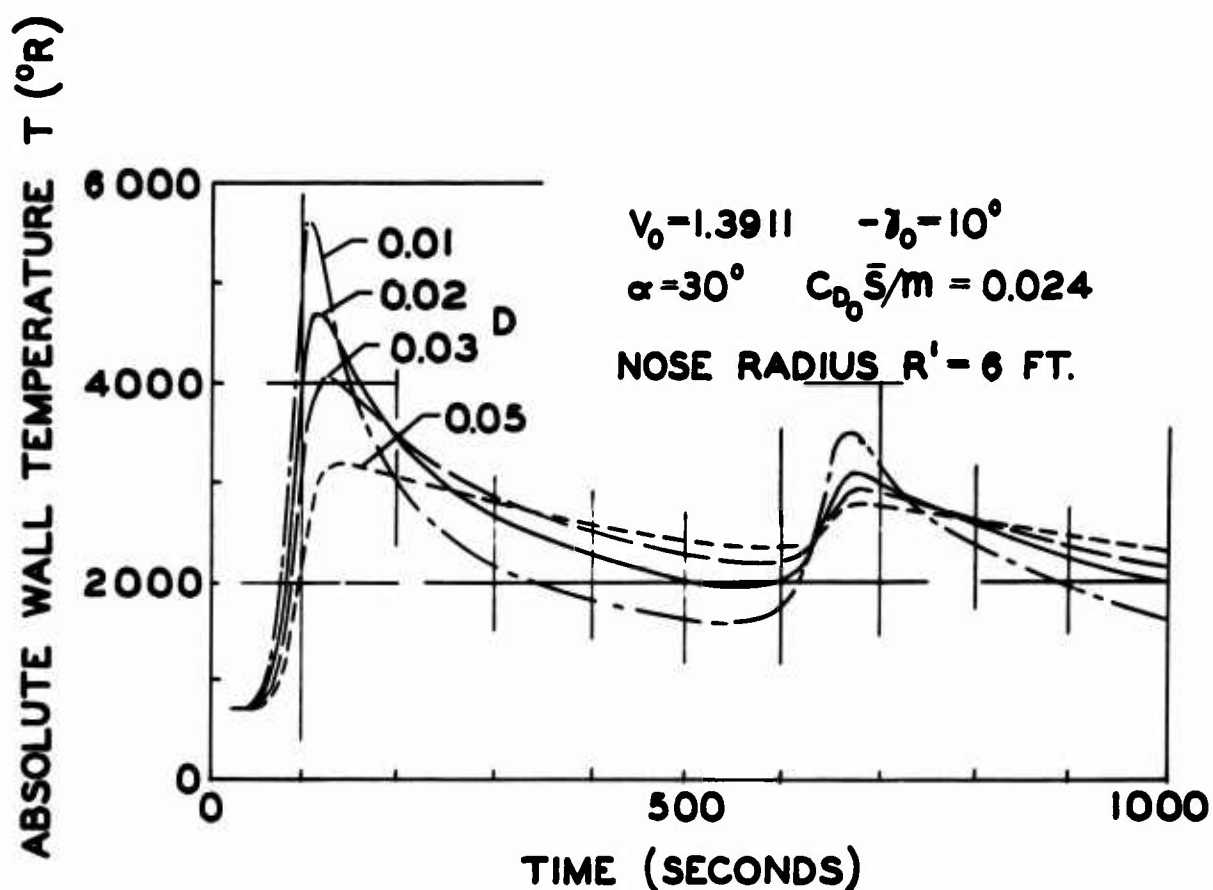
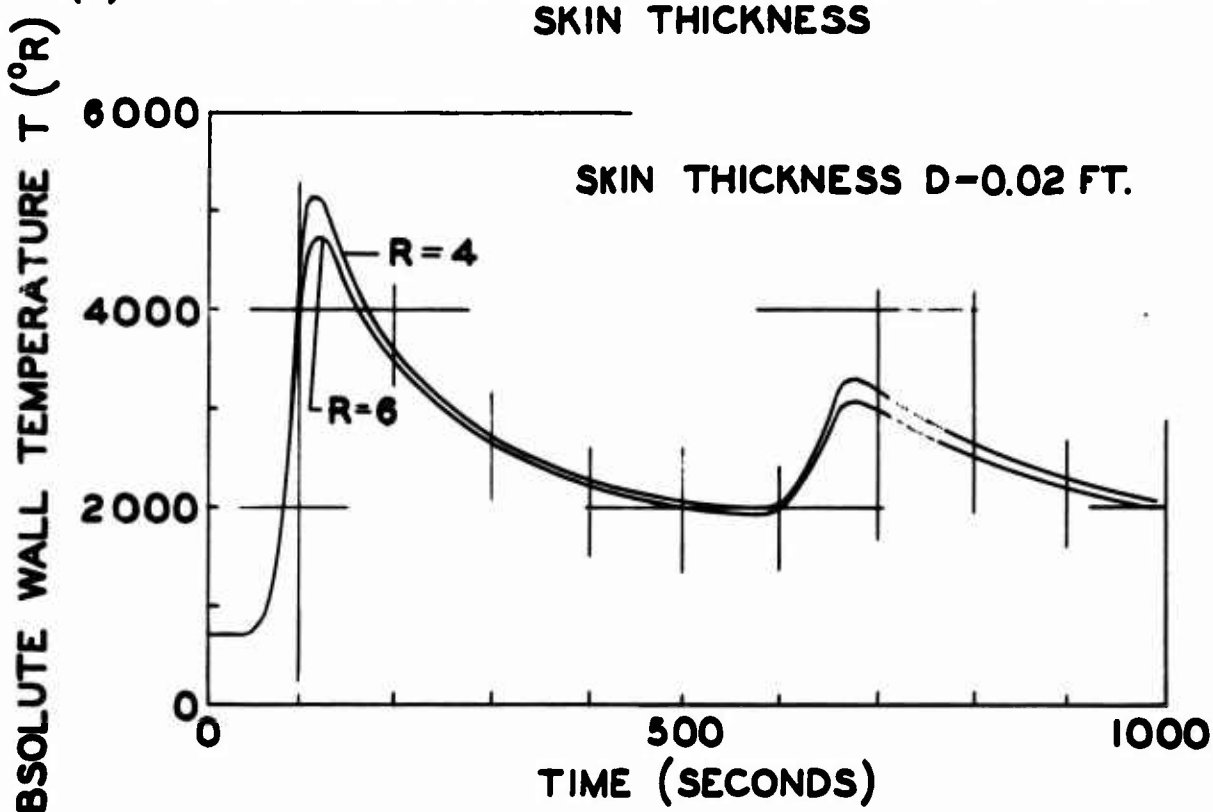


FIG. 9 EFFECT OF ENTRY ANGLE AT MAXIMUM LIFT  
ON DECELERATION AND TEMPERATURE

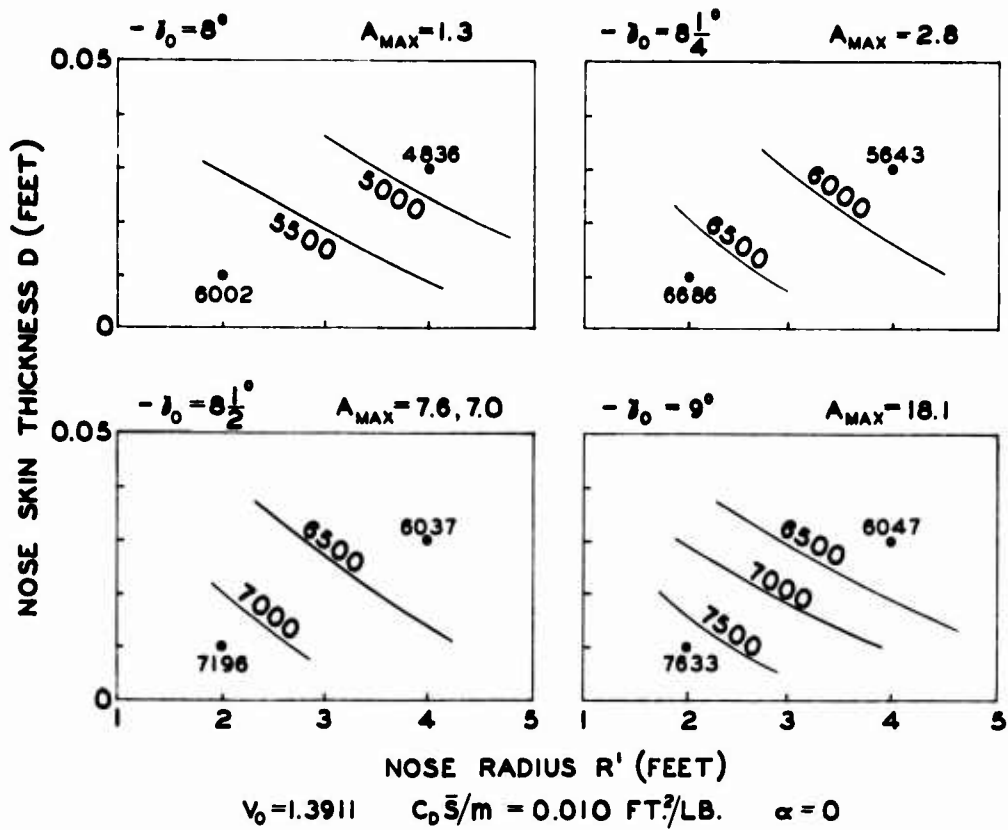


(a) THE EFFECT ON WALL TEMPERATURE OF NOSE SKIN THICKNESS



(b) THE EFFECT ON WALL TEMPERATURE OF NOSE RADIUS

FIG. 10 ENTRY AT MAXIMUM LIFT:  
WALL TEMPERATURE - TIME HISTORIES



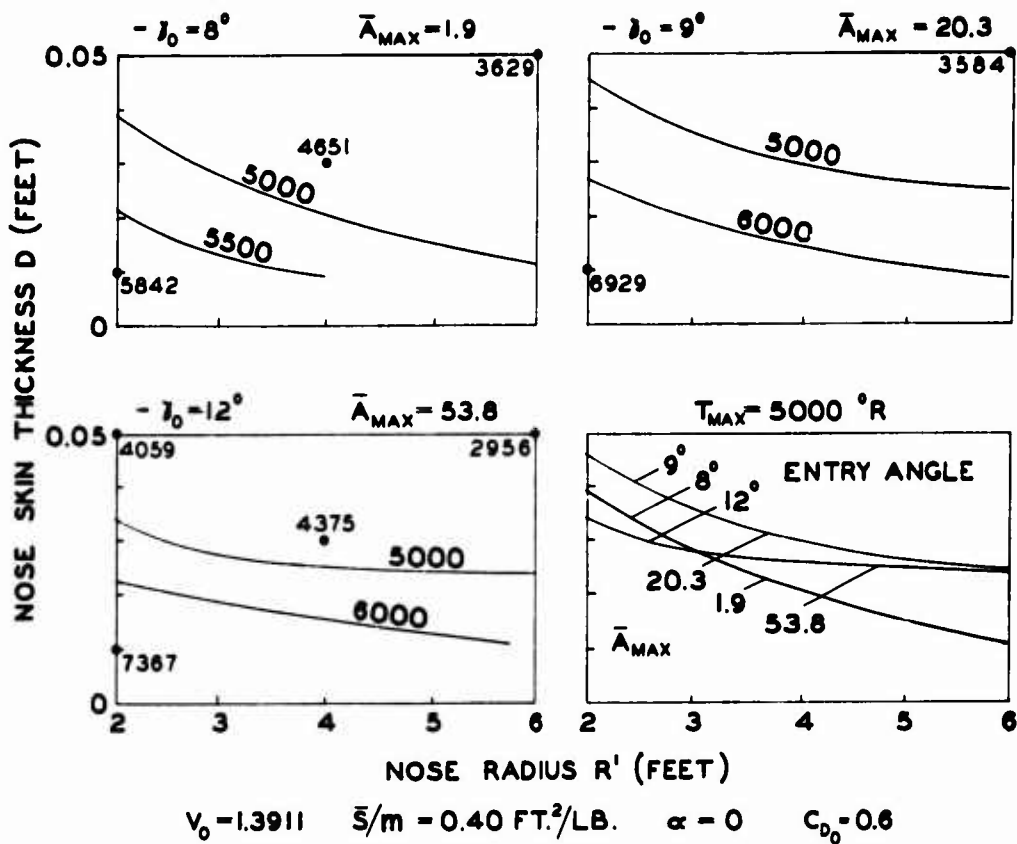


FIG. 13  
NOSE GEOMETRY AND PEAK WALL TEMPERATURE:  
EFFECT OF STEEP ENTRY AT ZERO LIFT

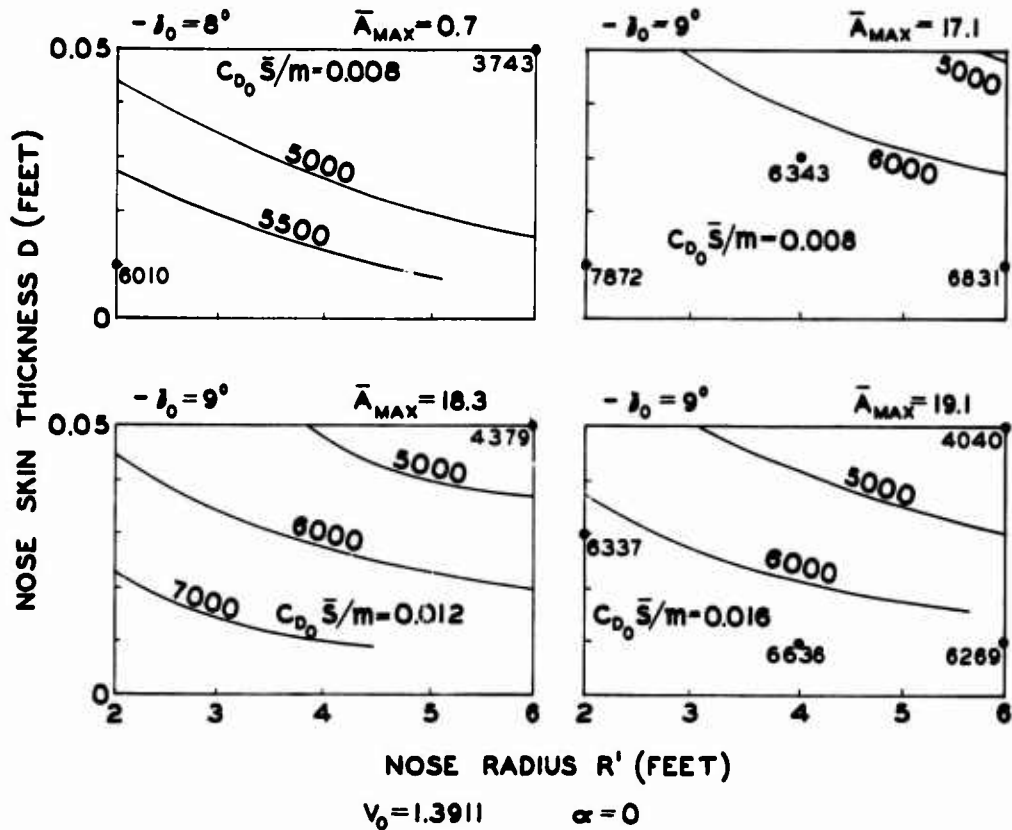


FIG. 14  
NOSE GEOMETRY AND PEAK WALL TEMPERATURE:  
EFFECT OF  $m/C_0 \bar{S}$  AT ZERO LIFT

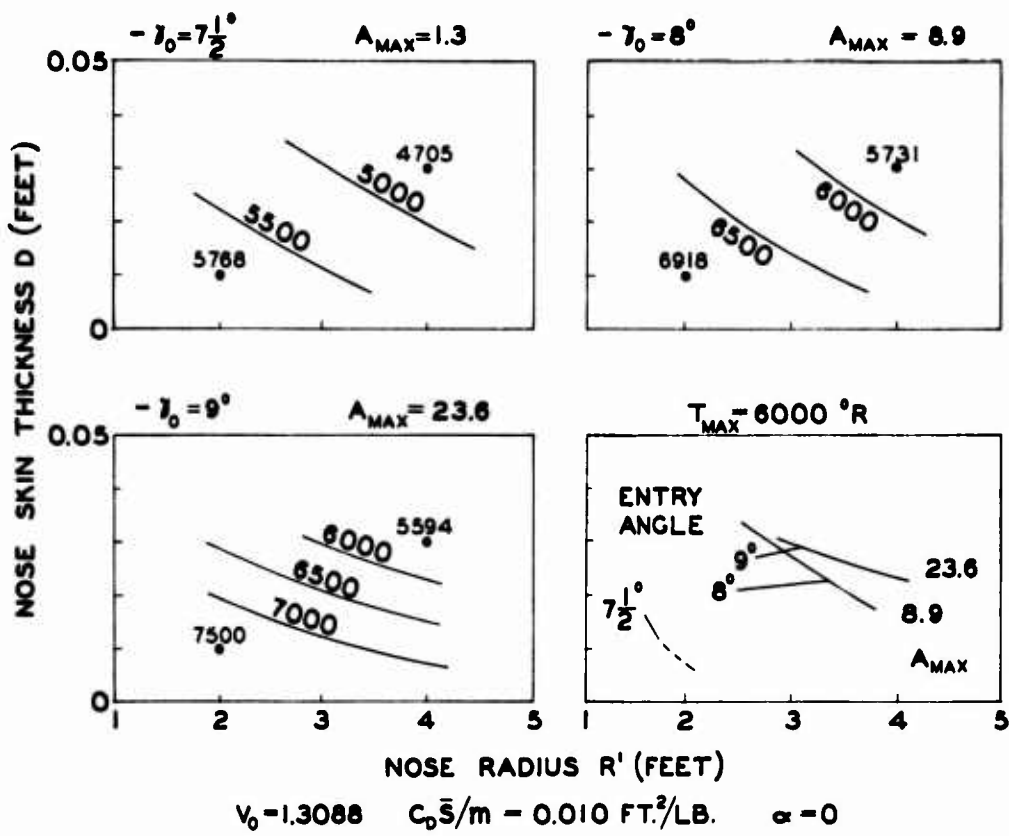


FIG. 15  
NOSE GEOMETRY AND PEAK WALL TEMPERATURE:  
EFFECT OF ENTRY ANGLE AT ZERO LIFT

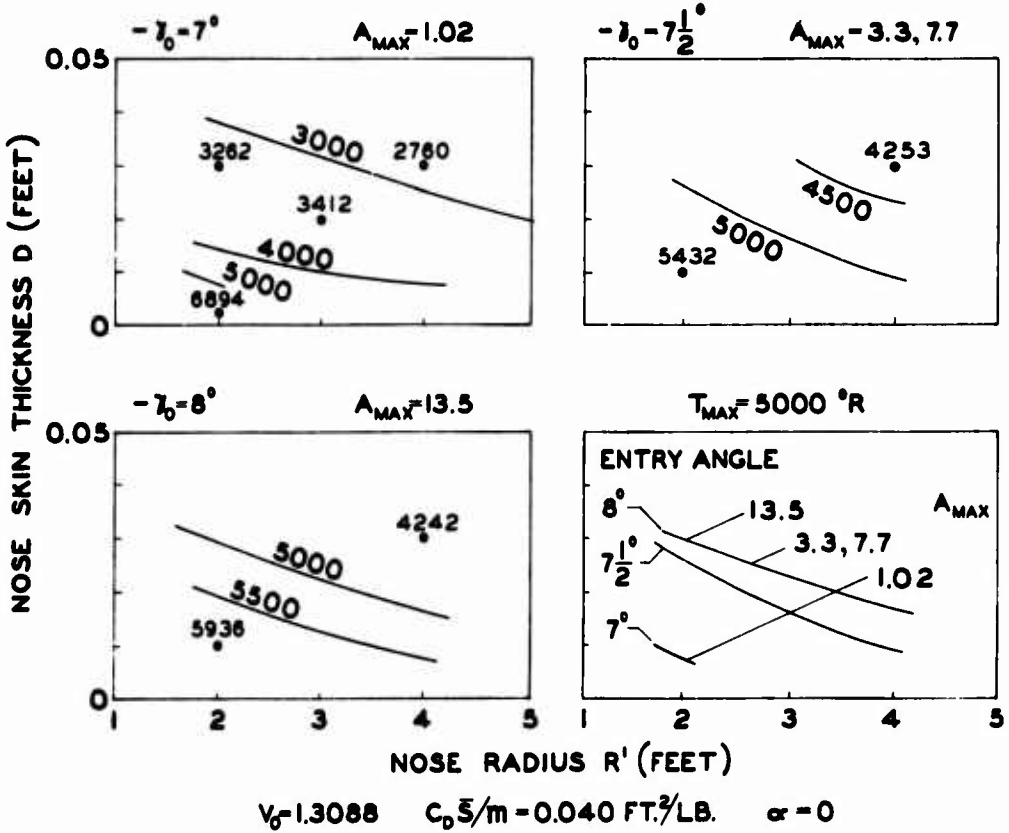


FIG. 16  
NOSE GEOMETRY AND PEAK WALL TEMPERATURE:  
EFFECT OF ENTRY ANGLE AT ZERO LIFT

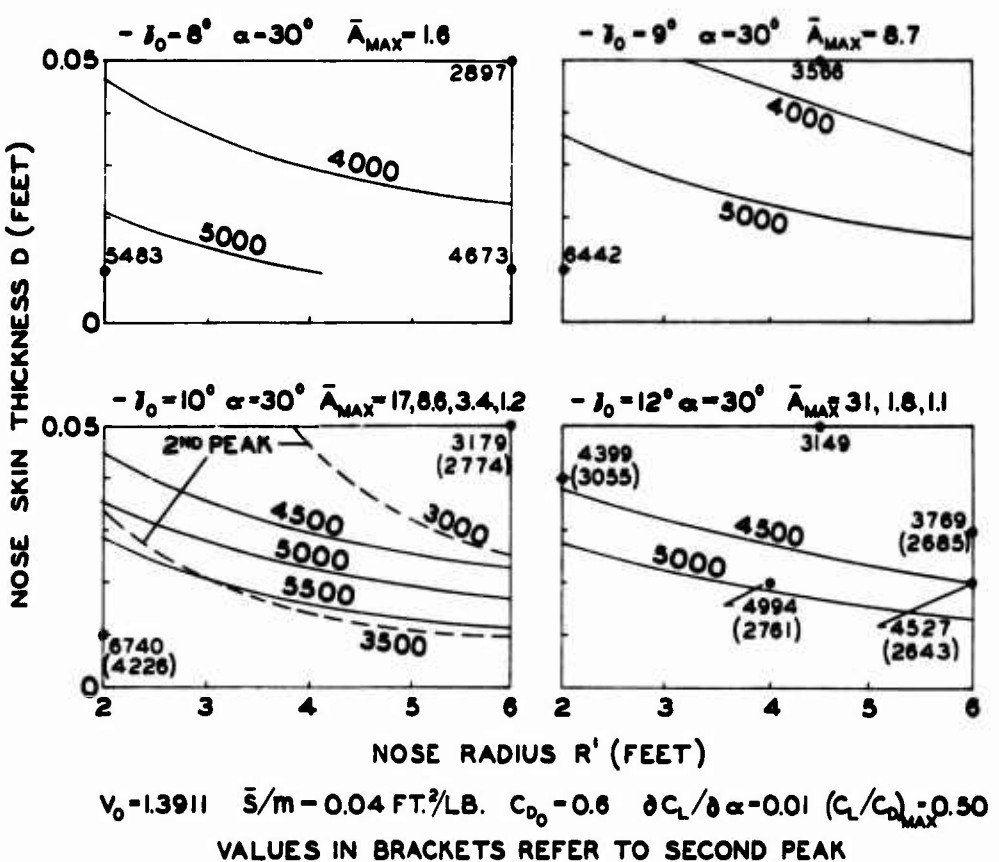
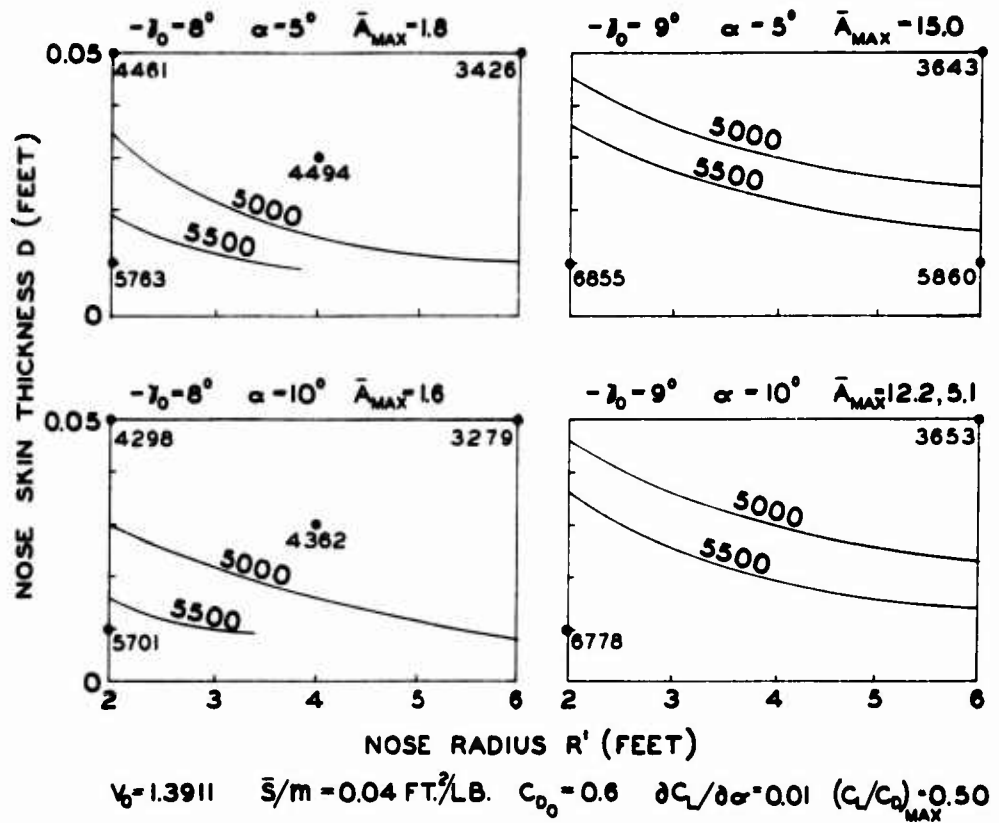


FIG. 18

NOSE GEOMETRY AND PEAK WALL TEMPERATURE:  
MAXIMUM LIFT ENTRY